# Chapter 14
# Meteorology, Climatology, and Upper Atmospheric Composition for Infrasound Propagation Modeling


**Douglas Drob**

**Abstract** Over the last decade, there have been improvements in global data assimilation capabilities of the lower, middle, and upper atmosphere. This includes mesoscale specification capabilities for the troposphere. This chapter provides an overview of both operational and basic scientific research specifications of the atmosphere from the ground to the thermosphere that are available for the calculation of infrasound propagation characteristics. This review is intended for scientific experts, nonexperts, researchers, educators, and policy makers alike. As atmospheric specifications for the lower and middle atmosphere are now readily available, less uncertain, and also described in other chapters of this book, some additional emphasis is placed on the challenges associated with upper atmospheric specifications for modeling thermospherically ducted infrasound propagation. Otherwise, no particular emphasis is placed on any one atmospheric specification system or institutional data provider; nor anyone particular infrasound propagation application, i.e., local, regional, global, man-made, or natural.

## 14.1 Overview

In order to detect, locate, and discriminate energetic impulsive events via infrasound accurately, it is important to know how acoustic waveforms evolve as they propagate away from a source and are subsequently observed by seismic networks and infrasound arrays. In the case of infrasound, this requires specification of the time-dependent transfer function between the source and receivers. This time-dependent transfer function is determined by the acoustic signal characteristics, atmospheric properties, and instrument response functions of the detectors. Unlike seismic waveforms, for identical events and source to receiver configurations, the observed infrasound signal characteristics (e.g., amplitude and travel time) are highly variable due to the time dependence of the atmosphere (Rind 1978; Le Pichon et al. 2002; Drob et al. 2003). Propagation is also highly anisotropic due to the effects of winds which

D. Drob
Naval Research Laboratory, 4555 Overlook Avenue, Washington, DC 20375, USA
e-mail: douglas.drob@nrl.navy.mil



A. Le Pichon et al. (eds.), *Infrasound Monitoring for Atmospheric Studies*,
https://doi.org/10.1007/978-3-319-75140-5_14

can vary markedly with range and altitude for a given propagation path (Georges and Beasley 1977; Garcés et al. 1998).

Over the last decade, there has been considerable progress in specifying the real-time state of the atmosphere (e.g., Bauer et al. 2015), as well as in understanding the consequences for infrasound propagation. These include improvements in understanding signal travel times, amplitudes, and waveform durations, including the spatial extent of the geometric infrasound shadow zones (Evers and Haak 2007; Green et al. 2011; Evers et al. 2012; Hedlin and Drob 2014). Several recent studies show that it is now possible to explain the relevant features of recorded data tropospheric and stratospheric arrivals well by including physics-based parameterizations of subgrid-scale atmospheric internal waves in conjunction with today's standard operational meteorological data assimilation products (e.g., Chunchuzov et al. 2011; Lalande and Waxler 2016). For a number of reasons described in this chapter, corresponding success in modeling observed thermospheric infrasound propagation characteristics remains somewhat illusive (e.g., Assink et al. 2013; Lonzaga et al. 2015).

### *14.1.1 Atmospheric Specifications*

Traditionally, the regions of the atmosphere are categorized by the vertical temperature gradients, i.e., the troposphere, stratosphere, mesosphere, and thermosphere. The local average temperature profile and altitudes of these regions are shown in Fig. 14.1. The exact altitudes vary somewhat with latitude and day of year. For this chapter, the atmospheric specifications available for infrasound propagation modeling are the easiest to describe considering three basic regions: the lower atmosphere from the earth's surface to 35 km, the middle atmosphere from 35 to 85 km, and the upper atmosphere from 85 to 450 km. The meteorology of these regions are each controlled by somewhat different physical processes, and each also has very different observational coverage. At the top of the atmosphere near ~400 km, the average distance traveled by gas particles between collisions becomes equal to the density scale height (the distance required for the density to decrease by a factor of $1/e \sim 36\%$) and thus no longer supports classically defined acoustic propagation.

For this chapter, a key distinction should be made between atmospheric data assimilation systems which produce 'analyses', and that of Numerical Weather Prediction (NWP) models which produce 'forecasts'. Analyses are the best possible estimate of the present and/or past state of the atmosphere given all available observations. A forecast is the best possible estimate of the future state of the atmosphere based on a theoretical extrapolation of analyses forward in time via a physics-based first-principles NWP model. These physics-based models integrate the four-dimensional (4D) meteorological equations of fluid motion with various parameterizations for the different subgrid-scale physical processes of the atmosphere.

One of the most important factors in providing an accurate weather forecast is producing the most accurate analysis possible. These analyses are generated

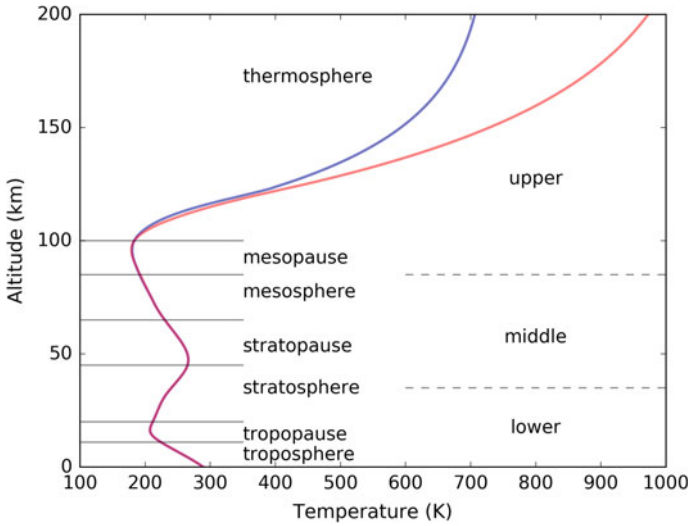


**Fig. 14.1** Various regions of the atmosphere for the nomenclature in this chapter. The blue curve corresponds to low Extreme Ultraviolet (EUV) solar flux conditions (low sunspot number) and the red curve to high EUV solar flux conditions (high sunspot number)

at regular time intervals (typical every 3- to 6-h) via a data assimilation system. The system compiles the many available observations over the analysis update interval to produce an atmospheric specification which is physically self-consistent with the physics of the forecast model. These analyses are also sometimes called nowcasts or hindcasts. The self-consistency of the available noisy, disparate, and sometimes even instrument calibration biased atmospheric observations with the physical laws of the atmospheric forecast model is obtained by adding an adjoint constraint operator term to a traditional statistical field estimation cost function operator (e.g., Daley 1993). In other words, the analysis field cost function operators include both a geophysical model error covariance term to account for uncertainties in the atmospheric model, and an observational error covariance term to account for the measurement uncertainties of the available observations.

For the atmosphere below ∼35 km, given a good atmospheric model and a sufficient number of observations, today's atmospheric analysis fields are even statistically more accurate than any one single individual observation such as a radiosonde profile (e.g. Edwards 2010). This results from the fact that multiple overlapping and/or adjacent observations can work together with the geophysical constraints provided by the numerical weather prediction forecast model to mitigate measurement noise and instrument calibration biases. Furthermore, unlike an instantaneous local point measurement, operational NWP systems provide vital information about any local range dependent gradients that can be import to infrasound propagation modeling, as well as the time evolution of the atmosphere.

While the notion of ensemble numerical weather forecasting has been around for at least 25 years (e.g., Toth et al. 1997), a recent advance is the notion of ensemble

atmospheric data assimilation which provides improved knowledge about the statistical distribution of analyses based on the measurement uncertainties, as well as the statistical distribution of the forecasts to better account for uncertainties in atmospheric model physics (Zhang and Pu 2010; Houtekamer and Zhang 2016). Almost every atmospheric global data assimilation system today also utilizes a technique called four-dimensional data assimilation (4D-Var) (e.g. Courtier et al. 1994; Rabier et al. 2000). Here, the time evolution of all of the observations, typically on the order of $2 \times 10^6$ new independent measurements within a 3- to 6-h window, are reconciled with the time evolution of the atmosphere over that time interval through a simplified version of the numerical forecast model. The most advanced systems utilize hybrid techniques involving ensemble, four-dimensional data assimilation (4D-EnVar) (e.g., Lorenc 2003; Bonavita et al. 2016). Although only analyses are typically considered relevant for infrasound propagation modeling calculations, because the atmosphere is always changing utilization of archived 3-h forecasts products provide vital information between analysis update cycles (usually 6 h), and are superior to linear interpolation of 6- or 12-h analysis updates.

### *14.1.2 Statistical Ensembles and Internal Waves*

A ubiquitous feature of the atmosphere is the internal subgrid-scale buoyancy oscillations known as gravity waves (Hines 1960; Gossard and Hooke 1975). These are not to be confused with gravitational waves (Abbott et al. 2016). These atmospheric oscillations have wave periods from ∼10 to 180 min, vertical wavelengths from 1 to 20 km, and horizontal wavelengths ranging from ∼15 to >100 km. For additional details, see Fritts and Alexander (2003). Even with the recent technological advances, owing to the spatiotemporal scales of these waves, it is impractical to deterministically measure and resolve them with any fidelity beyond a certain resolution limit in a comprehensive sense, i.e., at every possible location and time. Furthermore, these subgrid-scale phenomena must be filtered from the analysis fields during the operational data assimilation process to avoid the generation of spurious numerical artifacts when integrating the forecast model forward in time (Daley 1993).

The significance of small-scale (mid-frequency) internal atmospheric gravity waves for infrasound propagation has been clearly elucidated (e.g., Millet et al. 2007; Kulichkov et al. 2010; Lalande and Waxler 2016). It should be noted that the European Center for Medium-Range Weather Forecasting (ECMWF) ensemble analysis states presented in Smets et al. (2015) to reconcile differences between observed and modeled infrasound propagation characteristics generally represent perturbations (or random realizations) of the synoptic scale manifold of the analysis fields, i.e., the spatiotemporally resolvable but uncertain large- and medium-scale meteorological features. Here, the specifications utilized are only provided for two universal times each day (i.e., at 12-h intervals). This differs from consideration of the mid- and high-frequency atmospheric gravity wave perturbations, which have wave periods between ∼10 min and 3-h (e.g., Fritts and Alexander 2003; Drob et al. 2013; Preusse

et al. 2014). For the purposes of infrasound propagation calculations, these unresolved atmospheric perturbations can be represented as a stochastic noise field that is superimposed on the resolved background field; much in the same way that turbulence is parameterized in aerodynamic drag calculations. Unlike the large scale background atmospheric manifold, these waves influence infrasound propagation characteristics through subgrid scale refraction effects akin to weak forward scattering. These topics are described in more detail in other chapters of this book (Waxler and Assink 2019; Chunchuzov and Kulichov 2019; Cugnet et al. 2019).

Independent of infrasound propagation, these internal waves are important players in the mass, momentum, and energy budgets of the atmosphere as they transport momentum and energy into the middle and upper atmosphere through their dissipation, as well as by enhancing the eddy transport of ozone, water vapor, and heat. All operational NWP systems include gravity wave parameterizations (e.g., Ern et al. 2006; Orr et al. 2010; Geller et al. 2013). The spatial resolution of numerical forecast systems such as at the European Center for Medium-Range Weather Forecasting (ECMWF) is now even theoretically capable of deterministically resolving some of the larger scale and lower frequency internal gravity wave components. Recent detailed independent validation studies by Preusse et al. (2014) and Jewtoukoff et al. (2015) however compared the resolved gravity waves in ECMWF to observations and found that the resolved gravity waves generated in ECMWF are not yet always accurately specified and sometimes differed in their spectral characteristics from the observations. The major difficulty with the deterministic resolution of internal gravity waves in NWP analysis systems, as well as by the tuning of stochastic subgrid-scale gravity parameterizations (e.g., Warner and McIntyre 2001) is that the amplitudes, phases, and spectral characteristics of these internal oscillations vary significantly as function of time with the ambient atmospheric conditions. In particular, this is the result of time-dependent nonlinear source intermittency that is on the order of an hour or so (e.g., Hertzog et al. 2012; Costantino et al. 2015). As differences in atmospheric gravity wave parameterization schemes result in different analysis and forecast specifications in the upper stratosphere and mesosphere where observations become sparse, the measurement and characterization of the local, regional, and global evolution of these waves is an active area of scientific research.

## 14.2 The Challenge of Atmospheric Seismology

Although infrasound science can be considered as atmospheric seismology, there are also many important differences with traditional seismology. In seismology, the construction of solid earth models for seismic waveform synthesis is motivated by applications such as oil, gas, and mineral exploration, seismic hazard assessments, and even arms control treaty monitoring. By contrast, recent advances in atmospheric specification capabilities are motivated by applications such as commerce, agriculture, aviation, severe weather warnings, volcanic ash plume monitoring, and defense applications that are completely unrelated to infrasound propagation.

In seismology, the only viable means to obtain measurements to create and validate solid Earth models is through seismic waveform technologies. The Earth's atmosphere can however be measured through a wide variety of different in situ and remote sensing methods that are totally independent of infrasound. The in situ techniques include ground stations, ocean buoys, radiosondes, aviation-based sensors, and sounding rockets. The remote sensing techniques include ground-based vertical profilers and global satellite measurement techniques which span across the entire electromagnetic spectrum from the EUV wavelengths to Ultra high Frequency (UHF) radio waves. As the result of having multiple overlapping techniques available present atmospheric measurements are easy to intercompare and are thus well validated.

In the context of atmospheric specifications available for infrasound propagation modeling, there is an excellent understanding of the fundamental properties of the atmosphere, particularly for the lower and middle portions. The main challenge however is that unlike the solid earth, the atmosphere is time-dependent over scales from several minutes to several years. Figure 14.2 shows the approximate time and length scales for the pertinent meteorological phenomenology that determines the variability of the atmosphere that infrasound signals propagate through. A proper understanding of this time dependence is vital to understanding the limitations of present day atmospheric specifications for the calculation of infrasound propagation characteristics, and ultimately the physical limitations of infrasound waveform technologies as compared to other geophysical monitoring techniques, or in conjunction with them.

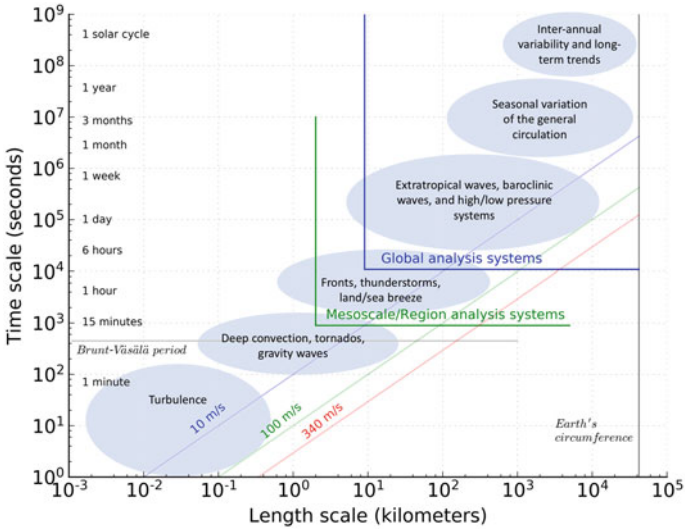


**Fig. 14.2** Spatiotemporal variability of various atmospheric phenomena, including the present resolution of various regional (green) and global (blue) atmospheric data analysis and numerical weather prediction products (After Bauer et al. 2015, and others)

**Table 14.1** Geophysical infrasound monitoring applications

| Application | Network size[a] | Waveguide[b] | Timeliness[c] |
|---|---|---|---|
| Rayleigh wave coupling | L, R, G | R, S, T | N, H |
| Atmospheric remote sensing | R, G | S, T | N, H, T, C |
| Volcano phenomenology | L, R, G | R, S, T | N, H, T |
| Bolides | R, G | R, S, T | N, H |
| Microbarms/Microseisms | R, G | S, T | N, H, T, C |
| Landslides/Avalanches | L, R | R, S | N, H |
| Thunder and lightning | L, R | R, S | N, H |
| Explosion monitoring | L, R, G | R, S, T | N, H, T, C |
| Structural acoustics | L, R | R, S | N, H |

[a]L—Local (10–100 km), R—Regional (100—750 km), G—Global (>750 km)
[b]R—Troposphere (<15 km), S—Stratosphere (15–70 km), T—Thermosphere (>70 km)
[c]N—Nowcast, H—Hindcast, T—Time series, C—Climatology

Table 14.1 shows the relevant infrasound network size, acoustic waveguides, and required temporal availability for several representative infrasound monitoring applications. The scale sizes of infrasound networks can be grouped into three general categories: local, regional, and global. While the timescales for these infrasound applications to be practical vary from several minutes to several days, the time delay and temporal resolution of the corresponding atmospheric specifications needed for infrasound propagation modeling also vary from a nowcast, hindcast, and continuous historical time series, to simple climatological averages.

The nature of the infrasound application also determines the required vertical extent of the atmospheric specifications needed to model the observed infrasound waveform characteristics (such as amplitude, frequency content, and signal duration). For near-field and regional infrasound propagation calculations over distances of no more that ∼150 km, atmospheric specifications only up to about 35 km altitude are usually needed. At these distances, consideration of topographical variations is also usually required in the vicinity of mountainous regions (Lacanna et al. 2014). For infrasound propagation calculations over distances greater than ∼150 km (and including global propagation), atmospheric specifications that include the stratosphere up to ∼70 km are usually required. Consideration of the intermediate topographic variations may or may not be required. Atmospheric specifications up to ∼140 km are required if thermospheric arrivals are to be considered in regional and global scale propagation calculations (e.g., Marcillo et al. 2013; Blom et al. 2015). Infrasound ducted in the thermosphere is however subject to significant attenuation above ∼100 km. Thus to accurately model thermospheric propagation, specification of the atmospheric composition (described later in Sect. 14.5.1) is also required in addition to winds $U$ and temperatures $T$, resulting in additional challenges.

## 14.3 Lower Atmospheric Specifications

With respect to infrasound propagation below ~35 km, the atmosphere is the most well resolved and understood region. Highly detailed and accurate atmospheric specifications are readily available from two classes of operational numerical weather prediction systems: global scale and regional mesoscale systems. Below the tropopause, the atmosphere's meteorology is coupled to the air/land/sea interface through processes such as heat exchange, evaporation, and precipitation. Secondary effects include mountain range blocking and even surface roughness. Both aloft and near the surface, the physics of state changes between the solid, liquid, and gas phases of $H_2O$ is one of the most important meteorological processes involved. Incoming short-wave solar radiation responsible for surface heating and outgoing long-wave radiation responsible for surface cooling are also important factors. Additional information can be found in any meteorology textbook (e.g., Fleagle and Businger 1981; Warner 2010).

The various global analysis fields are based on the observations from the integrated global observing system coordinated by the World Meteorology Organization (WMO). To generate the operational analyses $\sim 2 \times 10^6$, new independent observations are made every few hours over the globe by ground- and space-based sensors. These observations are gathered, shared, filtered, and processed by the various atmospheric data assimilation systems to produce the near-real-time analyses. A detailed list of the operational space-based sensors and ground-based stations in this network is available at the WMO website (https://www.wmo-sat.info/oscar/), as well as the many validation and product verification reports by the NWP system operators (e.g., Dee et al. 2011; Bosilovich et al. 2015). An interesting historical account of the evolution of numerical weather prediction and today's global network of weather observations is provided by Edwards (2010).

### *14.3.1 Global*

Today, it is typical for available atmospheric analysis systems to have horizontal resolutions up to $10 \times 10$ km (~0.125°) that extend from the ground well into the middle atmosphere, and that are updated approximately every 3–6 h. Unlike a decade ago, these resolutions are now expressed in terms of kilometers rather than degrees. A partial list of the major present day operational NWP systems is provided in Table 14.2. This table also includes the acronyms and websites for these NWP centers.

Given the spatiotemporal correlations shown in Fig. 14.2, as the resolution of atmospheric specifications increases spatially, it is then equally important to simultaneously consider the temporal resolution of the specifications too. In other words, sufficient temporal resolution of the background fields is required when performing infrasound propagation calculations to properly specify the location of the resolved atmospheric structures that are resolved by the meteorological data analysis system.

**Table 14.2** Representative numerical data assimilation and operational weather prediction systems

| Center | System | Global resolution[1] | Vertical levels | Model top |
|---|---|---|---|---|
| ECMWF[a] | Integrated Forecast System (IFS) | 9 × 9 km (T1279) | 137 | 0.01 hPa (80 km) |
| NCEP[b] | Global Forecast System (GFS) | 13 × 13 km (T1534) | 64 | 0.27 hPa (55 km) |
| UKMO[c] | Unified Model (UM) | 17 × 17 km (T1025) | 80 | 0.01 hPa (80 km) |
| JMA[d] | Global Spectral Model (GSM) | 18 × 18 km (T959) | 100 | 0.01 hPa (80 km) |

[1]T—maximum spherical harmonic spectral order
[a]European Center for Medium-Range Weather Forecasting (ECMWF), http://www.ecmwf.int
[b]National Center for Environmental Prediction (NCEP), http://www.ncep.noaa.gov
[c]United Kingdom Meteorology Office (UKMO), http://www.metoffice.gov.uk
[d]Japan Meteorology Agency (JMA), http://www.jma.go.jp/jma/indexe.html

The temporal resolution required is proportional to the spatial scale of those structures. For example, as synoptic scale waves and weather fronts can travel by as much as 200 to 300 km (~2° to 4°) over the course of 6- to 12-h, particularly in the stratosphere, it makes no sense to utilize 18 × 18 km resolution atmospheric specifications if they do not correspond to within an hour or so of the origin time of a given event.

With respect to vertical resolution, almost all of these modern systems utilize a hybrid-sigma vertical coordinate system which follows the Earth's topography near the surface, and slowly transitions to constant pressure levels in the lower stratosphere. Typical vertical resolutions are several 10 s of meters near the surface and a few kilometers near the upper boundaries. The altitudes of these vertical model levels also vary as a function of latitude, longitude, and time, so the atmospheric specifications for a given event must be interpolated to a fixed geometric coordinate system for utilization in infrasound propagation codes. A simple yet effective approach is to interpolate and extrapolate the available atmospheric fields to a fixed vertical altitude grid with respect to the Mean Sea Level (MSL), and specifically including altitudes below the Earth's surface such as near the Tibetan plateau, Greenland, or Antarctic ice shelf. The virtual atmospheric grid points that are below the Earth's surface can then be explicitly be masked out with a separate digital terrain model that better matches the resolution of the infrasound propagation calculations.

### *14.3.2 Regional/Mesoscale Specifications*

To provide improved spatiotemporal resolution for severe storm front tracking and tracer transport monitoring of volcanic ash, remarkable advances in regional mesoscale atmospheric specifications have occurred in the past decade. Systems

with up to $2 \times 2$ km resolution are being transitioned into operations, with $13 \times 13$ km $\times$ 1-h resolutions specifications up to 35 km altitude being the legacy standard. New systems such as the NCEP High Resolution Rapid Refresh (HRRR) provide regional meteorological specifications over the Continental United States (CONUS) and Alaska with $3 \times 3$ km resolution, with outputs at 15-min cadences for some of the fields. For reasons described in Sect. 14.4, compared to the global systems, these regional system have a slightly lower upper boundary typically near a constant pressure level of ~20 hPa (~25 km). Similarly, the UKMO mesoscale system produces $2.2 \times 2.2$ km resolution fields every 3 h, as well as at $1.5 \times 1.5$ km region for local regions. The JMA operates a mesoscale regional analysis system with $5 \times 5$ km horizontal resolution that has 50 vertical levels up to 22 km, and hourly output resolution; as well as a local forecast model with $2 \times 2$ km resolution on 60 levels up to ~20 km.

To properly resolve these meteorological length and timescales, today's mesoscale systems integrate the fully compressible non-hydrostatic fluid equations (e.g., Honda et al. 2005; Saito et al. 2007). Some of the global scale systems described earlier even now include non-hydrostatic compressible terms. The highest resolution mesoscale systems are even basically capable of resolving large convective lengths scales (e.g. Prein et al. 2015). Unlike present infrasound propagation codes which compute propagation characteristics from the first- or second-order linear and/or nonlinear perturbation expansion to the fluid equations, these non-hydrostatic solutions are calculated through the first-order fully resolved Navier–Stokes equations (e.g., Giraldo and Restelli 2008). However, the spatial extent and temporal resolution of these non-hydrostatic mesoscale models are still presently much greater than is needed to directly compute synthetic infrasound waveforms for compact impulsive infrasound events.

Today's mesoscale models can also provide highly resolved assimilative specifications of soil moisture, snow depth, and other meteorological dependent groundcover information relevant to infrasound monitoring. Such information is useful for diagnosing and understanding the spatiotemporal variability of infrasound sensor array response characteristics when dedicated soil moisture and snow depth sensors are not installed (or available) at an infrasound array, or at a potential infrasound source region. Specifically historical and/or near-real-time mesoscale specification of these may provide a better understanding of the causes of site specific differences in seismo-acoustic coupling (e.g., Walker et al. 2011; Hedlin and Walker 2013). As an example, by comparing hourly averaged infrasound pressure measurements across the of USArray Transportable Array (de Groot-Hedlin and Hedlin 2015) with hourly surface pressure specifications from the NCEP CONUS Rapid Updated Cycle (RUC) system for several months in 2013, it was possible to independently locate a number of problematic infrasound sensors in the network (R. Busby, personal communication).

## 14.4 Middle Atmospheric Specifications

Above the tropopause, the atmospheric meteorology begins to decouple from the sea surface temperatures, land–sea contrasts, and local terrain variations, and becomes predominately coupled to the global general circulation system of the stratosphere. This is why regional mesoscale systems generally do not extend well into the stratosphere. However, solar heating driven tides and waves of all scales generated in the lower atmosphere also propagate upward into the region; so the middle atmosphere is not completely uncoupled from the regional-scale dynamics of the lower atmosphere (Andrews et al. 1987). Physical processes such as ozone photochemistry and transport (e.g., Bednarz et al. 2016), heterogeneous ice chemistry (e.g., Solomon et al. 2015), and the momentum deposition from stationary and nonstationary subgrid-scale internal waves (e.g., Ern et al. 2016) are all important factors that govern the thermal structure and dynamics of the stratosphere.

Compared to the lower atmospheric specifications, civilian consumer demand for around the clock real-time middle atmospheric specifications and forecasts is basically nonexistent. The stratosphere can however influence the upper troposphere through mass, momentum, and energy transfer processes. The occurrence and phases of large stratospheric dynamical phenomena such as the Quasi-Biennial Oscillation (QBO) and Sudden Stratospheric Warmings (SSW) can be correlated with future meteorological patterns of the troposphere (Kidston et al. 2015). Thus, the middle atmospheric component of numerical weather prediction models provides a detailed upper boundary condition to resolve the influence of upper air steering currents and self-consistently compute the incoming solar UV and outgoing atmospheric infrared radiation. Another important reason for operational NWP systems to include a fully resolved middle atmosphere is to properly account for contaminating foreground atmospheric infrared and microwave radiation contributions in satellite-based remote sensing radiance observations of the lower atmosphere. All of the numerical weather prediction and atmospheric data assimilation systems which include a fully resolved middle atmosphere have improved forecast skill.

Middle atmospheric specifications associated with NWP systems are also integral to the international climate monitoring and middle atmospheric scientific research communities. Specifically, the middle atmosphere is susceptible to subtle changes in $CO_2$ composition (e.g., Funatsu et al. 2016), potential climatological changes in tropospheric dynamics (e.g., Garcia et al. 2016), and $O_3$ to man-made byproduct such as chlorofluorocarbons (CFCs) (e.g., Douglass et al. 2014). The tracking of injections and the subsequent fallout of volcanic aerosols in the stratosphere is also vital to understanding the impact that large volcanic eruptions have on the atmosphere and climate system (LeGrande et al. 2016).

These reasons motivate governmental investments in what are also known as reanalysis systems. One such system is the Goddard Earth Observing System (Version 5) GEOS5 which is used to produce the Modern-Era Retrospective analysis for Research and Applications, version 2 (MERRA2) analysis products (Bosilovich et al. 2015; Coy et al. 2016). Similarly, other major NWP centers (see Butchart et al.

2011) such as ECMWF Dee et al. 2011, JMA Harada et al. 2016, and NCEP (Saha et al. 2014) also produce reanalysis products for independent validation, comparison, and research. These reanalysis efforts also provide benchmarks and opportunities to develop and validate improved model physics for future operational NWP systems. The various reanalysis products from these systems are made publicly accessible for scientific research purposes, but for a number reasons (e.g., production cost, data archive, and distribution requirements) most available reanalysis products lag real-time by a month to several years, and may have slightly lower resolutions than operational numerical weather prediction forecast data products. One difference between these reanalysis fields and operational system analysis fields is that the underlying model assumptions are held constant over the entire multi-decade time interval; unlike the operational analysis archives where model resolution, physics, and the number of vertical levels routinely change.

## 14.5 Upper Atmospheric Specifications

Presently, there are no fully operational numerical weather prediction systems that encompass the lower thermosphere. This is the result of two main issues: the first is the cost and difficulty in making routine measurements of the region, the second is the lack of operational requirements as the result of strong direct economic and societal demands. A third factor is that the fundamental physics of the region is sufficiently different from the lower and middle atmosphere such that the basic *single fluid* meteorological conservation equations for mass, momentum, and energy can no longer be utilized.

To properly model the atmosphere above ~100 km, a viable meteorological forecast system must integrate the fully coupled *multispecies* transport equations, including the first-order effects of the global scale ionospheric electrodynamics (e.g., Rees 1989; Schunk and Nagy 2009). This is a consequence of the EUV photodissociation of $O_2$ producing atomic oxygen (O), subsequent EUV ionization of O and $O_2$ which produces the ionosphere, as well as the lack of turbulent mixing above about ~105 km, all resulting in O becoming the dominant species above ~175 km. The presence of an ionosphere in the Earth's magnetic field results in electrodynamics effects such as joule heating, aurora heating, and horizontal ion-neutral momentum coupling that have first-order influences on the *meteorology* of the upper atmosphere. As a result, the existing system of governing equations utilized in lower and middle atmospheric numerical weather prediction models cannot be extended from 75 to 250 km by simply adding additional model levels and constraining those results to match operational observations of the upper atmosphere.

Despite these challenges efforts to operationalize, the NOAA Whole Atmospheric Model (WAM) (https://esgf.esrl.noaa.gov/projects/wam_ipe/) for space weather applications is an active area of both basic and applied research. First-principles models of these processes have however existed for many years. One of the first non-assimilative models that can self-consistently represent these processes on a global

scale is the National Center for Atmospheric Research (NCAR), Thermosphere-Ionosphere-Electrodynamics General Circulation Model (TIE-GCM) (Richmond et al. 1992) and the Thermosphere-Ionosphere-Mesosphere-Electrodynamics General Circulation Model (TIME-GCM) (Roble and Ridley 1994). Other coupled thermosphere-ionosphere-electrodynamic models include the Coupled Thermosphere-Ionosphere-Plasmasphere-Electrodynamics (CTIPe) model (Fuller-Rowell and Rees 1980; Fuller-Rowell et al. 2002) and the Global Ionosphere Thermosphere Model (GITM) (Ridley et al. 2006). Recently a new class of 'Whole' atmospheric models are striving to account for these processes in a self-consistent manner with the lower and middle atmosphere (see Roble 2000). Examples are the NOAA Whole Atmosphere Model (WAM) (Akmaev 2011), the Hamburg Model for the Neutral and Ionized Atmosphere (HAMMONIA) (Schmidt et al. 2006), the NCAR Whole Atmosphere Community Climate Model-Extended (WACCMX) model (Liu et al. 2010), and the Ground-to-Topside Model of Atmosphere and Ionosphere for Aeronomy (GAIA) model (Jin et al. 2011). Unlike assimilative NWP systems, these models are generally free running, i.e., they are only driven by external forcings of the system at the upper and lower boundaries, and not constrained with real-time operational data above 85 km. Where they extend to lower altitudes and overlap with existing middle atmospheric analyses, they can be 'nudged 'or constrained (e.g., Stauffer and Seaman 1990) so that the observed meteorological variations there can be extrapolated (via theoretical considerations) into the thermosphere above (Marsh 2011; Siskind and Drob 2014; Sassi and Liu 2014).

While being a promising approach for the specification of the upper atmosphere between 85 and 200 km, it may be some time before operational systems are ready for utilization by independent third parties for uses such as infrasound monitoring. The limiting factor here is the lack of an adequate and truly *operational* global satellite- and ground-based network of sensors for the atmospheric region from 85 to 250 km. Today, only basic scientific research satellite mission datasets and ground-based research measurements exist for model validation and research-to-operation purposes. Thus, near-term infrasound propagation calculations must either rely on the extrapolation of data from below 85 km to lower thermospheric altitudes via the first-principles physics-based models, serendipitously coincident basic upper atmospheric research measurement, and/or empirical climatological models.

Unfortunately, unlike lower atmospheric radiosonde profiles, no one single upper atmospheric measurement technique simultaneously measures both winds and temperatures between 65 and 140 km and, in particular, across all ground ranges from an infrasound source to an infrasound detector. While measurements from co-located ground-based sensor suites of LIDARS and MF RADARs (Liu et al. 2002; Franke et al. 2005; Suzuki et al. 2010) can be combined to approach this capability, there are only a few research facilities where such instrument suites exist. Furthermore, these combine atmospheric observations are only limited in applicability to within a few 100 km of the measurement points, as well as to within about an hour or so in time. LIDAR observations are also generally limited to altitudes below ~105 km and to cloud free nighttime only conditions, but there are some exceptions. These research facilities are however ideal for validating future operational upper atmospheric

specifications systems, as well as for developing and calibrating new measurement techniques for future space-based systems, which are all required to operate global real-time NWP systems encompassing the thermosphere.

Presently, most infrasound propagation codes that consider thermospheric propagation utilize the observationally based Naval Research Laboratory (NRL) empirical upper atmospheric climatologies, the Mass Spectrometer Incoherent Scatter Radar Model Extended (NRLMSISE-00) (Picone et al. 2002), and the Horizontal Wind Model (HWM14) (Drob et al. 2015). These are part of the International Committee on Space Research (COSPAR) International Reference Atmosphere (CIRA). These empirical models are based on 50 years of satellite- and ground-based research observations. To combine the many available disparate research measurements into a complete observational based time-dependent global specification, these models utilize the simplest form of data assimilation known as observational function fitting (Daley 1993).

The end-user FORTRAN subroutines for these empirical upper atmospheric climatologies can be obtained at https://map.nrl.navy.mil/map/pub/nrl/HWM/HWM14/ and https://map.nrl.navy.mil/map/pub/nrl/NRLMSIS/NRLMSISE-00/. The input parameters to these empirical models are the day of year, universal time, latitude, longitude, altitude, the daily, and 81-day averaged measures of $F_{10.7}$ $cm^{-1}$ solar radio wave flux (a proxy for solar EUV radiation), and the $A_p$ geomagnetic activity index. These indices can be obtained for dates back to 1956 and in real time from http://www.swpc.noaa.gov/products-and-data. Otherwise no inputs of external observational data sets are needed by a user to run the MSIS and HWM client subroutines. The model outputs are winds, temperature, density, pressure, and atmospheric composition as a function of the specified latitude, longitude, altitude, day of year, and universal time. By matching these empirical models to the upper boundary conditions of the near-real-time lower and middle atmospheric specifications near ~75 km, Drob et al. (2003, 2010a) developed a simple approach to generate hybrid range- and time-dependent whole atmospheric specifications from the ground to space (0 to 200 km) that can be utilized to model thermospherically ducted infrasound propagation.

For infrasound propagation calculations above ~85 km, with longitudinal wavenumbers only up to $l = 3$, and latitudinal wave numbers only up to $n = 8$, a present limitation of the NRL empirical models is their low spectral resolution. Temporally the empirical models include the annual and semiannual seasonal variations, as well as the diurnal, semidiurnal, and terdiurnal migrating tidal harmonics, with the annual and semiannual seasonal modulations thereof. While this seems surprisingly crude as compared to the lower- and middle- atmospheric specifications, the meteorology of the upper atmosphere is primarily denominated by direct cyclical in situ forcing by EUV solar radiation (e.g., Roble 1983), deep westward migrating solar heating driven tidal modes propagating upward from below (e.g., Forbes and Wu 2006), and in situ geomagnetic forcing (e.g., Fuller-Rowell et al. 1994). The predominant seasonal variations of the thermosphere are phased locked with the earth's orbit around the sun, and the tidal variations with the earth rotation, with secondary modulations by geomagnetic forcing and solar variability. On average, these

variations account for the majority of the meteorology of the upper atmosphere, about ∼75–85% depending on altitude, field, and season. Being repeatable from year to year and day to day, these can be reasonably well parameterized with 50 years of observations and an appropriate set of basis functions. See Picone et al. (2002); Drob et al. (2015) and references therein for additional details. For some infrasound calculations, this is generally sufficient.

In the upper mesosphere and lower thermosphere, there is however a significant amount of regional variability, ∼25–35% that can not be readily resolved by empirical models (e.g., Liu 2016). Such variations will have consequences for precise modeling of thermospheric infrasound propagation characteristics for specific events. Most, but not all of this variability resides in the amplitudes and phases of the migrating and non-migrating solar tides. These variations result from longitudinal variations in water vapor in the troposphere and ozone in the stratosphere where the solar heating migrating tidal variations are forced (e.g., Forbes and Wu 2006). The day-to-day tidal variability can be on the order of 30% in tidal amplitude and 1–3 h in phase, but depends on latitude, altitude, and seasons. As a consequence, the westward migrating solar semidiurnal (12-h) tidal amplitudes in HWM in the 90 to 120 km region at mid-to-high latitudes can be underestimated by as much as 30–40 m/s on any given day, however there is little disagreement when the observations are averaged over a month or so.

Although available nudged and free running first-principles thermosphere and whole atmospheric general circulation models have sufficient spatiotemporal resolution to theoretically resolve this day-to-day variability, these present *physics-based* models can also exhibit regional biases in a number of fields depending on altitude, latitude, and day of year. Integrated over longer propagation paths, these systematic biases thus have the potential to be non-negligible in the infrasound propagation modeling error budget. In summary, presently available upper atmospheric specifications for infrasound propagation calculations of thermospheric infrasound propagation are rudimentary at best as compared to the fidelity and accuracy of lower- and middle- atmospheric specifications. There are however efforts unrelated to infrasound propagation that may eventually remedy this situation in the near future.

### *14.5.1 Upper Atmospheric Composition*

As mentioned, EUV photo-disassociation of molecular oxygen results in atomic oxygen becoming the dominant atmospheric compositional species above ∼175 km. This has important consequences for the atmospheric sound speed above ∼100 km through the ratio of specific heats ($\gamma$) and mean molecular mass ($\bar{m}$).

The global average number density profiles ($n_i$) of the seven major upper atmospheric species from the NRLMSISE-00 model (over the typical range solar EUV flux conditions from the minimum to the maximum of the sunspot cycle) is shown in Fig. 14.3. Much like winds and temperatures, upper atmospheric composition varies

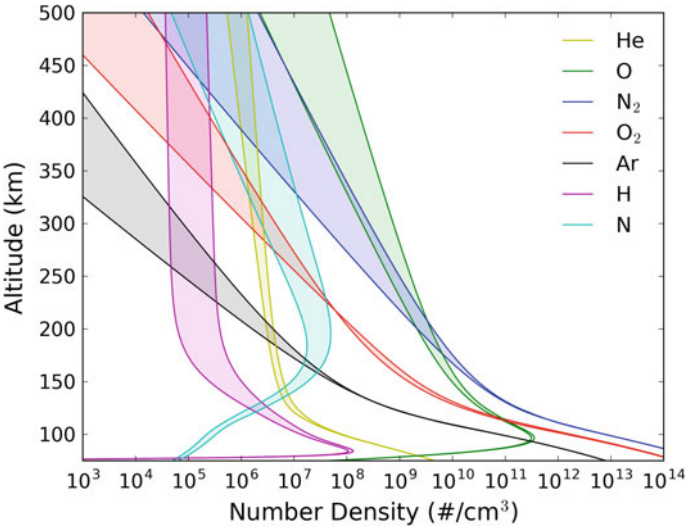


**Fig. 14.3** Observed global average atmospheric number density of the seven major upper atmospheric constituents from the MSIS empirical model

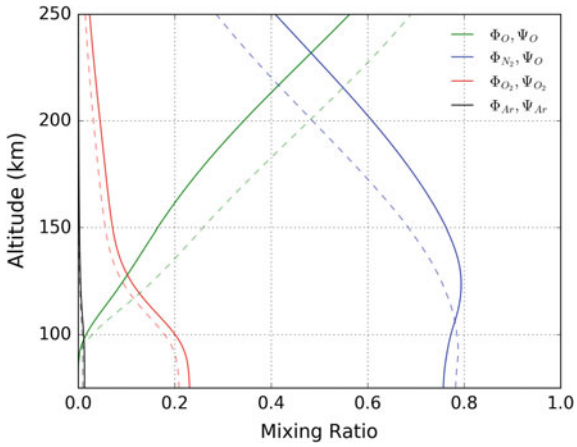


**Fig. 14.4** Global average major individual species volume $\Phi_i$ (solid) and mass $\Psi_i$ (dashed) mixing ratios (minimum solar cycle conditions) for molecular nitrogen ($N_2$; blue), molecular oxygen ($O_2$; red), and atomic oxygen (O, green)

somewhat as a function of latitude, day of year, local time, and geomagnetic activity. Such variations are reasonably well represented within the NRLMSIS-00 and theoretical first-principles models (Hedin 1987; Rishbeth and Müller-Wodarg 1999; Pedatella et al. 2016).

To highlight the significance of these compositional changes of the upper atmosphere in contrast to the lower thermosphere, the corresponding upper atmospheric volume $\Phi_i$ and mass $\Psi_i$ mixing are shown in Fig. 14.4. The volume mixing ratio of the $i$th species is defined as $\Phi_i = n_i / \sum_j n_j = n_i/N = P_i/P$, where $P_i = n_i kT$ is the partial pressure, $P = nkT$ is the total atmospheric pressure, and $n$ is the total number

density. The mass mixing ratio of the $i$th species is defined as $\Psi_i = n_i m_i / \sum_j m_j n_j$. The calculations shown assume that all the atmospheric constituents have the same average kinetic temperature which is reasonably below ~400 km. As seen in Fig. 14.4, departures from the constant major species composition mixing ratios of the lower and middle atmosphere; $\Phi_{N_2} = 0.7808$, $\Phi_{O_2} = 0.2093$, and $\Phi_{Ar} = 0.0009$ (see Mohr et al. 2012) begin to occur at about ~100 km.

Ignoring second-order vibrational and rotational collision effects important for high-frequency nonlinear acoustic propagation (e.g., Bass et al. 2007), the first-order expression for static sound speed is

$$c = \sqrt{\frac{\gamma RT}{\bar{M}}} = \sqrt{\frac{\gamma kT}{\bar{m}}} = \sqrt{\frac{\gamma P}{\rho}}, \tag{14.1}$$

where $\gamma = c_p / c_v$ (the ratio of specific heat at constant pressure $c_p$, to that at constant volume $c_v$), $R$ is the universal gas constant, and $\bar{M}$ average mass, $\bar{m}$ is the average molar mass, $k$ is the Boltzmann constant, and $\rho$ is the mass density. While the vertical atmospheric temperature profile must clearly be taken into account for infrasound propagation calculations, it is very common to assume that $\bar{m} = 28.9645$ g/mol and $\gamma = 1.4$ are both constants. This assumption results in the approximation $c \cong 20.0464\sqrt{T}$.

Changes in the upper atmospheric composition above ~85 km influence the static sound speed through changes in both $\bar{m}$ and $\gamma$. Note that both height integrated atmospheric pressure $P(z)$ and $\rho$ are also functions of $\bar{m}$. Given the number densities $n_i$, or mass mixing ratios $\Psi_i$, $\bar{m}$ can be calculated as

$$\bar{m} = \Big[ \sum_i \frac{\Psi_i}{m_i} \Big]^{-1} = \frac{\sum_i n_i m_i}{\sum_i n_i}. \tag{14.2}$$

Figure 14.5 shows the typical vertical variations of $\bar{m}(z)$ for the composition profiles shown in Fig. 14.3. From Chapman-Enskog theory (e.g., Gombosi 1994), a reasonable first-order approximation to calculate composition dependent specific heats ($c_p$,$c_v$) in the upper atmosphere is

$$c_p = \sum_m \frac{k}{2m_m}(2 + \Gamma_m)\Phi_m + \sum_a \frac{k}{2m_a}(2 + \Gamma_a)\Phi_a \tag{14.3}$$

$$c_v = \sum_m \frac{k}{2m_m}\Gamma_m \Phi_m + \sum_a \frac{k}{2m_a}\Gamma_a \Phi_a \tag{14.4}$$

where $m_m$ and $m_a$ are the individual molar masses of the respective molecular and atomic species; $\Gamma_m = 5$ and $\Gamma_a = 3$ the corresponding degrees of freedom of molecular and atoms; and $\Phi_m$ and $\Phi_a$ are the individual species volume mixing ratios for molecules and atoms. The corresponding altitude-dependent profile of $\gamma(z)$ for the low solar EUV flux conditions is also shown in Fig. 14.5.

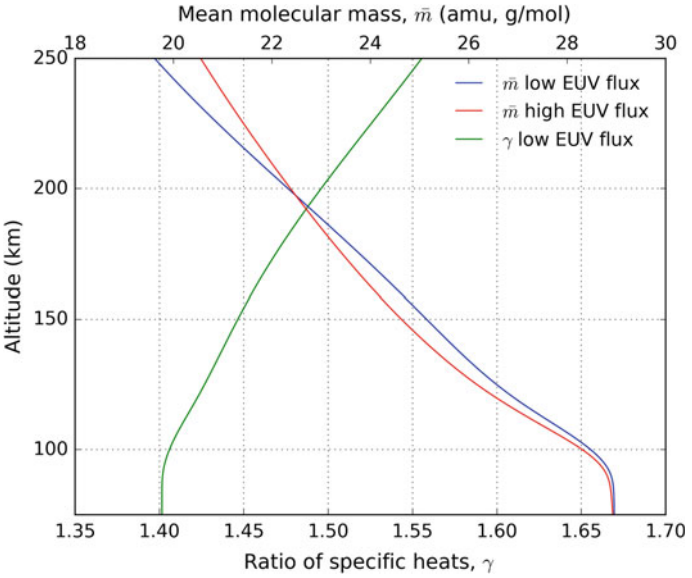


**Fig. 14.5** Typical altitude variations of $\bar{m}$ for low (blue) and high (red) solar EUV flux conditions, with $\gamma$ (green) shown for low EUV flux conditions

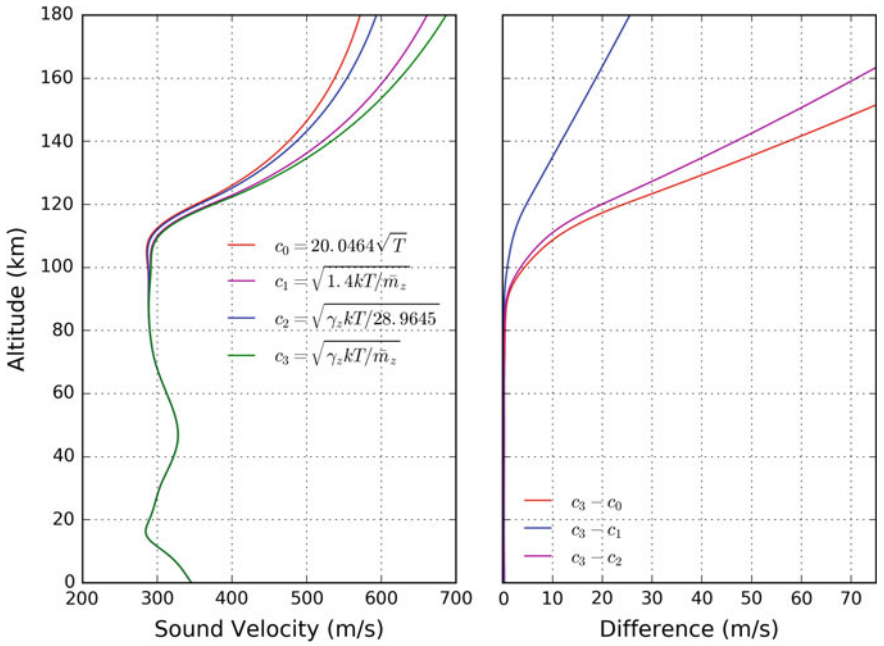


**Fig. 14.6** Comparison of static sound speed calculated with various assumptions for $\bar{m}$ and $\gamma$ in Eq. 14.1

The consequences of these composition variations in the calculation of the local vertical profiles of the static atmospheric sound speed is shown in Fig. 14.6. The right panel shows the difference between a temperature dependent only sound speed profile computed assuming constant $\bar{m}$ and $\gamma$, i.e., $c_0 = 20.0464\sqrt{T}$ (red), and one where $\bar{m}$ and $\gamma$ vary with altitude according to composition $c_3$ (green). The intermediate assumptions are indicated as $c_1$ (magenta) and $c_2$ (blue). The differences $c_3 - c_0$ (right panel, red) are on the order of 25 m/s near the turning points of thermospherically ducted infrasound (∼120 km) and in excess of ∼50 m/s above 150 km. Note that these are systematic biases that will accumulate over long propagation paths. Thus when estimating upper atmospheric wind speeds from infrasound travel times (e.g., Drob et al. 2010b; Assink et al. 2013) or calculating thermospheric infrasound propagation characteristics (e.g., Lonzaga et al. 2015; Sabatini et al. 2016), it is important to account for the atmospheric composition dependent variations of $\bar{m}$ and $\gamma$.

## 14.6 Conclusions

Over the last decade, there has been considerable progress in global data assimilation capabilities for the lower, middle, and upper atmosphere. There is a wide array of operational and basic research specifications of the atmosphere from the ground to the thermosphere that are available for the calculation of infrasound propagation characteristics. In infrasound propagation modeling calculations, with the dramatic increase in the spatial resolution of today's lower and middle atmospheric specifications, it is also important to consider in tandem the available temporal resolution of the specifications.

As compared to available meteorological specifications of the lower and middle atmosphere, observationally based specifications of the atmosphere above ∼85 km are much lower resolution and much more uncertain. This is primarily due to the lack of routine operational observations of the region driven by direct commercial applications. On the horizon, continuing basic research efforts to support space weather modeling activities should provide improvements in the specification of density, temperature, winds, and composition of the upper atmosphere, and eventually perhaps near-real-time global assimilation capabilities like for the lower and middle atmosphere. Such efforts will provide better atmospheric specifications for infrasound propagation calculations.

**Acknowledgements** This work was supported by the Chief of Naval Research.

## References

Abbott BP et al (2016) Observation of gravitational waves from a binary black hole merger. Phys Rev Lett 116(061):102. https://doi.org/10.1103/PhysRevLett.116.061102

Akmaev R (2011) Whole atmosphere modeling: connecting terrestrial and space weather. Rev Geophys 49(4)

Andrews DG, Holton JR, Leovy CB (1987) Middle atmosphere dynamics, vol 40. Academic press

Assink J, Waxler R, Frazier W, Lonzaga J (2013) The estimation of upper atmospheric wind model updates from infrasound data. J Geophys Res Atmos 118(19)

Bass HE, Hetzer CH, Raspet R (2007) On the speed of sound in the atmosphere as a function of altitude and frequency. J Geophys Res Atmos 112(D15)

Bauer P, Thorpe A, Brunet G (2015) The quiet revolution of numerical weather prediction. Nature 525(7567):47–55

Bednarz EM, Maycock AC, Abraham NL, Braesicke P, Dessens O, Pyle JA (2016) Future arctic ozone recovery: the importance of chemistry and dynamics. Atmos Chem Phys 16(18):12,159–12,176

Blom PS, Marcillo O, Arrowsmith SJ (2015) Improved bayesian infrasonic source localization for regional infrasound. Geophys J Int 203(3):1682–1693

Bonavita M, Hólm E, Isaksen L, Fisher M (2016) The evolution of the ECMWF hybrid data assimilation system. Q J R Meteorol Soc 142(694):287–303

Bosilovich M, Akella S, Coy L, Cullather R, Draper C, Gelaro R, Kovach R, Liu Q, Molod A, Norris P et al (2015) Merra-2: initial evaluation of the climate. NASA Technical report series on global modeling and data assimilation, NASA/TM-2015 104606

Butchart N, Charlton-Perez A, Cionni I, Hardiman S, Haynes P, Krüger K, Kushner P, Newman P, Osprey S, Perlwitz J et al (2011) Multimodel climate and variability of the stratosphere. J Geophys Res Atmos 116(D5)

Chunchuzov I, Kulichkov S (2019) Internal gravity wave perturbations and their impacts on infrasound propagation in the atmosphere. In: Le Pichon A, Blanc E, Hauchecorne A (eds) Infrasound monitoring for atmospheric studies, 2nd edn. Springer, Dordrecht, pp 551–590

Chunchuzov I, Kulichkov S, Popov O, Waxler R, Assink J (2011) Infrasound scattering from atmospheric anisotropic inhomogeneities. Izv Atmos Oceanic Phys 47(5):540–557

Costantino L, Heinrich P, Mzé N, Hauchecorne A (2015) Convective gravity wave propagation and breaking in the stratosphere: comparison between WRF model simulations and lidar data. Ann Geophys 33(9):1155–1171. https://doi.org/10.5194/angeo-33-1155-2015, http://www.ann-geophys.net/33/1155/2015/

Courtier P, Thépaut JN, Hollingsworth A (1994) A strategy for operational implementation of 4D-Var, using an incremental approach. Q J R Meteorol Soc 120(519):1367–1387

Coy L, Wargan K, Molod AM, McCarty WR, Pawson S (2016) Structure and dynamics of the quasi-biennial oscillation in MERRA-2. J Clim (2016)

Cugnet D, de la Camara A, Lott F, Millet C, Ribstein B (2019) Non-orographic gravity waves: representation in climate models and effects on infrasound. In: Le Pichon A, Blanc E, Hauchecorne A (eds) Infrasound monitoring for atmospheric studies, 2nd edn. Springer, Dordrecht, pp 827–844

Daley R (1993) Atmospheric data analysis, no 2. Cambridge university press

de Groot-Hedlin CD, Hedlin MA (2015) A method for detecting and locating geophysical events using groups of arrays. Geophys J Int 203(2):960–971

Dee D, Uppala S, Simmons A, Berrisford P, Poli P, Kobayashi S, Andrae U, Balmaseda M, Balsamo G, Bauer P et al (2011) The era-interim reanalysis: configuration and performance of the data assimilation system. Q J R Meteorol Soc 137(656):553–597

Douglass A, Strahan S, Oman L, Stolarski R (2014) Understanding differences in chemistry climate model projections of stratospheric ozone. J Geophys Res Atmos 119(8):4922–4939

Drob DP, Emmert JT, Meriwether JW, Makela JJ, Doornbos E, Conde M, Hernandez G, Noto J, Zawdie KA, McDonald SE et al (2015) An update to the horizontal wind model (HWM): the quiet time thermosphere. Earth Space Sci 2(7):301–319

Drob DP, Garcés M, Hedlin M, Brachet N (2010a) The temporal morphology of infrasound propagation. Pure Appl Geophys 167(4–5):437–453
Drob DP, Meier R, Picone JM, Garcés MM (2010b) Inversion of infrasound signals for passive atmospheric remote sensing. Infrasound monitoring for atmospheric studies. Springer, pp 701–731
Drob DP, Picone J, Garcés M (2003) Global morphology of infrasound propagation. J Geophys Res Atmos 108(D21)
Drob D, Broutman D, Hedlin M, Winslow N, Gibson R (2013) A method for specifying atmospheric gravity wavefields for long-range infrasound propagation calculations. J Geophys Res Atmos 118(10):3933–3943
Edwards PN (2010) A vast machine: computer models, climate data, and the politics of global warming. Mit Press
Ern M, Preusse P, Warner C (2006) Some experimental constraints for spectral parameters used in the Warner and Mcintyre gravity wave parameterization scheme. Atmos Chem Phys 6(12):4361–4381
Ern M, Trinh QT, Kaufmann M, Krisch I, Preusse P, Ungermann J, Zhu Y, Gille JC, Mlynczak MG, Russell III JM, Schwartz MJ, Riese M (2016) Satellite observations of middle atmosphere gravity wave absolute momentum flux and of its vertical gradient during recent stratospheric warmings. Atmos Chem Phys 16(15):9983–10,019. https://doi.org/10.5194/acp-16-9983-2016, http://www.atmos-chem-phys.net/16/9983/2016/
Evers L, Geyt A, Smets P, Fricke J (2012) Anomalous infrasound propagation in a hot stratosphere and the existence of extremely small shadow zones. J Geophys Res Atmos 117(D6)
Evers L, Haak H (2007) Infrasonic forerunners: exceptionally fast acoustic phases. Geophys Res Lett 34(10)
Fleagle RG, Businger JA (1981) An introduction to atmospheric physics, vol 25. Academic Press
Forbes JM, Wu D (2006) Solar tides as revealed by measurements of mesosphere temperature by the MLS experiment on UARS. J Atmos Sci 63(7):1776–1797
Franke S, Chu X, Liu A, Hocking W (2005) Comparison of meteor radar and Na Doppler lidar measurements of winds in the mesopause region above Maui, Hawaii. J Geophys Res Atmos 110(D9)
Fritts DC, Alexander MJ (2003) Gravity wave dynamics and effects in the middle atmosphere. Rev Geophys 41(1)
Fuller-Rowell TJ, Rees D (1980) A three-dimensional time-dependent global model of the thermosphere. J Atmos Sci 37(11):2545–2567
Fuller-Rowell T, Codrescu M, Moffett R, Quegan S (1994) Response of the thermosphere and ionosphere to geomagnetic storms. J Geophys Res Space Phys 99(A3):3893–3914
Fuller-Rowell T, Millward G, Richmond A, Codrescu M (2002) Storm-time changes in the upper atmosphere at low latitudes. J Atmos Solar Terr Phys 64(12):1383–1391
Funatsu BM, Claud C, Keckhut P, Hauchecorne A, Leblanc T (2016) Regional and seasonal stratospheric temperature trends in the last decade (2002–2014) from AMSU observations. J Geophys Res Atmos 121(14):8172–8185
Garcés MA, Hansen RA, Lindquist KG (1998) Traveltimes for infrasonic waves propagating in a stratified atmosphere. Geophys J Int 135(1):255–263
Garcia RR, López-Puertas M, Funke B, Kinnison DE, Marsh DR, Qian L (2016) On the secular trend of COx and CO2 in the lower thermosphere. J Geophys Res Atmos 121(7):3634–3644
Geller MA, Alexander MJ, Love PT, Bacmeister J, Ern M, Hertzog A, Manzini E, Preusse P, Sato K, Scaife AA et al (2013) A comparison between gravity wave momentum fluxes in observations and climate models. J Clim 26(17):6383–6405
Georges T, Beasley WH (1977) Refraction of infrasound by upper-atmospheric winds. J Acoust Soc Am 61(1):28–34
Giraldo FX, Restelli M (2008) A study of spectral element and discontinuous Galerkin methods for the Navier-Stokes equations in nonhydrostatic mesoscale atmospheric modeling: equation sets and test cases. J Comput Phys 227(8):3849–3877

Gombosi TI (1994) Gaskinetic theory, no 9. Cambridge University Press
Gossard EE, Hooke WH (1975) Waves in the atmosphere: atmospheric infrasound and gravity waves-their generation and propagation. Atmos Sci 2
Green DN, Vergoz J, Gibson R, Le Pichon A, Ceranna L (2011) Infrasound radiated by the Gerdec and Chelopechene explosions: propagation along unexpected paths. Geophys J Int 185(2):890–910
Harada Y, Kamahori H, Kobayashi C, Endo H, Kobayashi S, Ota Y, Onoda H, Onogi K, Miyaoka K, Takahashi K (2016) The JRA-55 reanalysis: representation of atmospheric circulation and climate variability. J Meteorol Soc Jpn Ser II 94(3):269–302. https://doi.org/10.2151/jmsj.2016-015
Hedin AE (1987) MSIS-86 thermospheric model. J Geophys Res Space Phys 92(A5):4649–4662
Hedlin MA, Drob DP (2014) Statistical characterization of atmospheric gravity waves by seismoacoustic observations. J Geophys Res Atmos 119(9):5345–5363
Hedlin MA, Walker KT (2013) A study of infrasonic anisotropy and multipathing in the atmosphere using seismic networks. Phil Trans R Soc A 371(1984):20110,542
Hertzog A, Alexander MJ, Plougonven R (2012) On the intermittency of gravity wave momentum flux in the stratosphere. J Atmos Sci 69(11):3433–3448
Hines CO (1960) Internal atmospheric gravity waves at ionospheric heights. Can J Phys 38(11):1441–1481
Honda Y, Nishijima M, Koizumi K, Ohta Y, Tamiya K, Kawabata T, Tsuyuki T (2005) A pre-operational variational data assimilation system for a non-hydrostatic model at the Japan meteorological agency: formulation and preliminary results. Q J R Meteorol Soc 131(613):3465–3475
Houtekamer PL, Zhang F (2016) Review of the ensemble kalman filter for atmospheric data assimilation. Monthly Weather Rev 144(12):4489–4532. https://doi.org/10.1175/MWR-D-15-0440.1
Jewtoukoff V, Hertzog A, Plougonven R, Adl Cámara, Lott F (2015) Comparison of gravity waves in the southern hemisphere derived from balloon observations and the ECMWF analyses. J Atmos Sci 72(9):3449–3468
Jin H, Miyoshi Y, Fujiwara H, Shinagawa H, Terada K, Terada N, Ishii M, Otsuka Y, Saito A (2011) Vertical connection from the tropospheric activities to the ionospheric longitudinal structure simulated by a new earth's whole atmosphere-ionosphere coupled model. J Geophys Res Space Phys 116(A1)
Kidston J, Scaife AA, Hardiman SC, Mitchell DM, Butchart N, Baldwin MP, Gray LJ (2015) Stratospheric influence on tropospheric jet streams, storm tracks and surface weather. Nature Geosci 8(6):433–440
Kulichkov S, Chunchuzov I, Popov O (2010) Simulating the influence of an atmospheric fine inhomogeneous structure on long-range propagation of pulsed acoustic signals. Izv Atmos Oceanic Phys 46(1):60–68
Lacanna G, Ichihara M, Iwakuni M, Takeo M, Iguchi M, Ripepe M (2014) Influence of atmospheric structure and topography on infrasonic wave propagation. J Geophys Res Solid Earth 119(4):2988–3005
Lalande JM, Waxler R (2016) The interaction between infrasonic waves and gravity wave perturbations: Application to observations using UTTR rocket motor fuel elimination events. J Geophys Res Atmos
Le Pichon A, Garcés M, Blanc E, Barthélémy M, Drob DP (2002) Acoustic propagation and atmosphere characteristics derived from infrasonic waves generated by the Concorde. J Acoust Soc Am 111(1):629–641
LeGrande AN, Tsigaridis K, Bauer SE (2016) Role of atmospheric chemistry in the climate impacts of stratospheric volcanic injections. Nature Geosci
Liu AZ, Hocking WK, Franke SJ, Thayaparan T (2002) Comparison of Na lidar and meteor radar wind measurements at Starfire Optical Range, NM, USA. J Atmos Solar Terr Phys 64(1):31–40

Liu HL, Foster B, Hagan M, McInerney J, Maute A, Qian L, Richmond A, Roble R, Solomon S, Garcia R et al (2010) Thermosphere extension of the whole atmosphere community climate model. J Geophys Res Space Phys 115(A12)

Liu HL (2016) Variability and predictability of the space environment as related to lower atmosphere forcing. Space Weather

Lonzaga JB, Waxler RM, Assink JD, Talmadge CL (2015) Modelling waveforms of infrasound arrivals from impulsive sources using weakly non-linear ray theory. Geophys J Int 200(3):1347–1361

Lorenc AC (2003) The potential of the ensemble Kalman filter for NWP–a comparison with 4D-Var. Q J R Meteorol Soc 129(595):3183–3203

Marcillo O, Arrowsmith S, Whitaker R, Anderson D, Nippress A, Green DN, Drob D (2013) Using physics-based priors in a Bayesian algorithm to enhance infrasound source location. Geophys J Int 353

Marsh DR (2011) Chemical–dynamical coupling in the mesosphere and lower thermosphere. Aeronomy of the earth's atmosphere and ionosphere. Springer, pp 3–17

Millet C, Robinet JC, Roblin C (2007) On using computational aeroacoustics for long-range propagation of infrasounds in realistic atmospheres. Geophys Res Lett 34(14)

Mohr PJ, Taylor BN, Newell DB (2012) CODATA recommended values of the fundamental physical constants: 2010. J Phys Chem Ref Data 41(4):043,109

Orr A, Bechtold P, Scinocca J, Ern M, Janiskova M (2010) Improved middle atmosphere climate and forecasts in the ECMWF model through a nonorographic gravity wave drag parameterization. J Clim 23(22):5905–5926

Pedatella N, Richmond A, Maute A, Liu HL (2016) Impact of semidiurnal tidal variability during SSWS on the mean state of the ionosphere and thermosphere. J Geophys Res Space Phys 121(8):8077–8088

Picone J, Hedin A, Drob DP, Aikin A (2002) NRLMSISE-00 empirical model of the atmosphere: Statistical comparisons and scientific issues. J Geophys Res Space Phys 107(A12)

Prein AF, Langhans W, Fosser G, Ferrone A, Ban N, Goergen K, Keller M, Tölle M, Gutjahr O, Feser F et al (2015) A review on regional convection-permitting climate modeling: demonstrations, prospects, and challenges. Rev Geophys 53(2):323–361

Preusse P, Ern M, Bechtold P, Eckermann SD, Kalisch S, Trinh QT, Riese M (2014) Characteristics of gravity waves resolved by ECMWF. Atmos Chem Phys 14(19):10,483–10,508. https://doi.org/10.5194/acp-14-10483-2014, http://www.atmos-chem-phys.net/14/10483/2014/

Rabier F, Järvinen H, Klinker E, Mahfouf JF, Simmons A (2000) The ECMWF operational implementation of four-dimensional variational assimilation. I: experimental results with simplified physics. Q J R Meteorol Soc 126(564):1143–1170

Rees MH (1989) Physics and chemistry of the upper atmosphere, vol 1. Cambridge University Press

Richmond A, Ridley E, Roble R (1992) A thermosphere/ionosphere general circulation model with coupled electrodynamics. Geophys Res Lett 19(6):601–604

Ridley A, Deng Y, Toth G (2006) The global ionosphere-thermosphere model. J Atmos Solar Terr Phys 68(8):839–864

Rind D (1978) Investigation of the lower thermosphere results of ten years of continuous observations with natural infrasound. J Atmos Terr Phys 40(10–11):1199–1209

Rishbeth H, Müller-Wodarg I (1999) Vertical circulation and thermospheric composition: a modelling study. Ann Geophys 17:794–805. Springer

Roble R (1983) Dynamics of the earth's thermosphere. Rev Geophys 21(2):217–233

Roble R (2000) On the feasibility of developing a global atmospheric model extending from the ground to the exosphere. Atmos Sci Across Stratopause 53–67

Roble R, Ridley E (1994) A thermosphere-ionosphere-mesosphere-electrodynamics general circulation model (time-GCM): equinox solar cycle minimum simulations (30–500 km). Geophys Res Lett 21(6):417–420

Sabatini R, Bailly C, Marsden O, Gainville O (2016) Characterization of absorption and nonlinear effects in infrasound propagation using an augmented burgers' equation. Geophys J Int 207(3):1432–1445

Saha S, Moorthi S, Wu X, Wang J, Nadiga S, Tripp P, Behringer D, Hou YT, Hy Chuang, Iredell M et al (2014) The NCEP climate forecast system version 2. J Clim 27(6):2185–2208

Saito K, Ishida JI, Aranami K, Hara T, Segawa T, Narita M, Honda Y (2007) Nonhydrostatic atmospheric models and operational development at JMA. J Meteorol Soc Jpn Ser II 85:271–304

Sassi F, Liu HL (2014) Westward traveling planetary wave events in the lower thermosphere during solar minimum conditions simulated by SD-WACCM-X. J Atmos Solar Terr Phys 119:11–26

Schmidt H, Brasseur G, Charron M, Manzini E, Giorgetta M, Diehl T, Fomichev V, Kinnison D, Marsh D, Walters S (2006) The HAMMONIA chemistry climate model: sensitivity of the mesopause region to the 11-year solar cycle and co2 doubling. J Clim 19(16):3903–3931

Schunk R, Nagy A (2009) Ionospheres: physics, plasma physics, and chemistry. Cambridge University Press

Siskind DE, Drob DP (2014) Use of NOGAPS-ALPHA as a bottom boundary for the NCAR/TIEGCM. Model Ionosphere Thermosphere Syst 171–180

Smets P, Evers L, Näsholm S, Gibbons S (2015) Probabilistic infrasound propagation using realistic atmospheric perturbations. Geophys Res Lett 42(15):6510–6517

Solomon S, Kinnison D, Bandoro J, Garcia R (2015) Simulation of polar ozone depletion: an update. J Geophys Res Atmos 120(15):7958–7974

Stauffer DR, Seaman NL (1990) Use of four-dimensional data assimilation in a limited-area mesoscale model. part I: experiments with synoptic-scale data. Monthly Weather Rev 118(6):1250–1277

Suzuki S, Nakamura T, Ejiri MK, Tsutsumi M, Shiokawa K, Kawahara TD (2010) Simultaneous airglow, lidar, and radar measurements of mesospheric gravity waves over japan. J Geophys Res Atmos 115(D24)

Toth Z, Kalnay E, Tracton SM, Wobus R, Irwin J (1997) A synoptic evaluation of the NCEP ensemble. Weather Forecast 12(1):140–153

Walker KT, Shelby R, Hedlin MA, Groot-Hedlin C, Vernon F (2011) Western us infrasonic catalog: Illuminating infrasonic hot spots with the USArray. J Geophys Res Solid Earth 116(B12)

Warner TT (2010) Numerical weather and climate prediction. Cambridge University Press

Warner C, McIntyre M (2001) An ultrasimple spectral parameterization for nonorographic gravity waves. J Atmos Sci 58(14):1837–1857

Waxler R, Assink J (2019) Propagation modeling through realistic atmosphere and benchmarking. In: Le Pichon A, Blanc E, Hauchecorne A (eds) Infrasound monitoring for atmospheric studies, 2nd edn. Springer, Dordrecht, pp 509–549

Zhang H, Pu Z (2010) Beating the uncertainties: ensemble forecasting and ensemble-based data assimilation in modern numerical weather prediction. Adv Meteorol 2010